

## Doping of a Plate-Type Acoustic Metamaterial

M. Mallejac,<sup>1, a)</sup> A. Merkel,<sup>2</sup> V. Tournat,<sup>1</sup> J-P. Groby,<sup>1</sup> and V. Romero-García<sup>1</sup>

<sup>1)</sup>*Laboratoire d'Acoustique de l'Université du Mans (LAUM), UMR 6613,  
Institut d'Acoustique - Graduate School (IA-GS), CNRS, Le Mans Université,  
France*

<sup>2)</sup>*Université de Lorraine, CNRS, IJL, F-54000 Nancy, France*

This supplementary material describes the transfer matrix method (TMM) used in the analytical calculations, the experimental set-up, and the inverse procedure used to extract the effective properties from the scattering parameters of the Plate-Type Acoustic Metamaterials (PAM). The lossless case of a 20 plates metamaterials is shown as well as videos illustrating the doping phenomena on a complex shape medium, here the "LAUM"-shaped medium.

---

<sup>a)</sup>Electronic mail: matthieu.mallejac@univ-lemans.fr

## I. EXPERIMENTAL SET-UP

Figures 1(a-d) show some photographs of the experimental set-up.

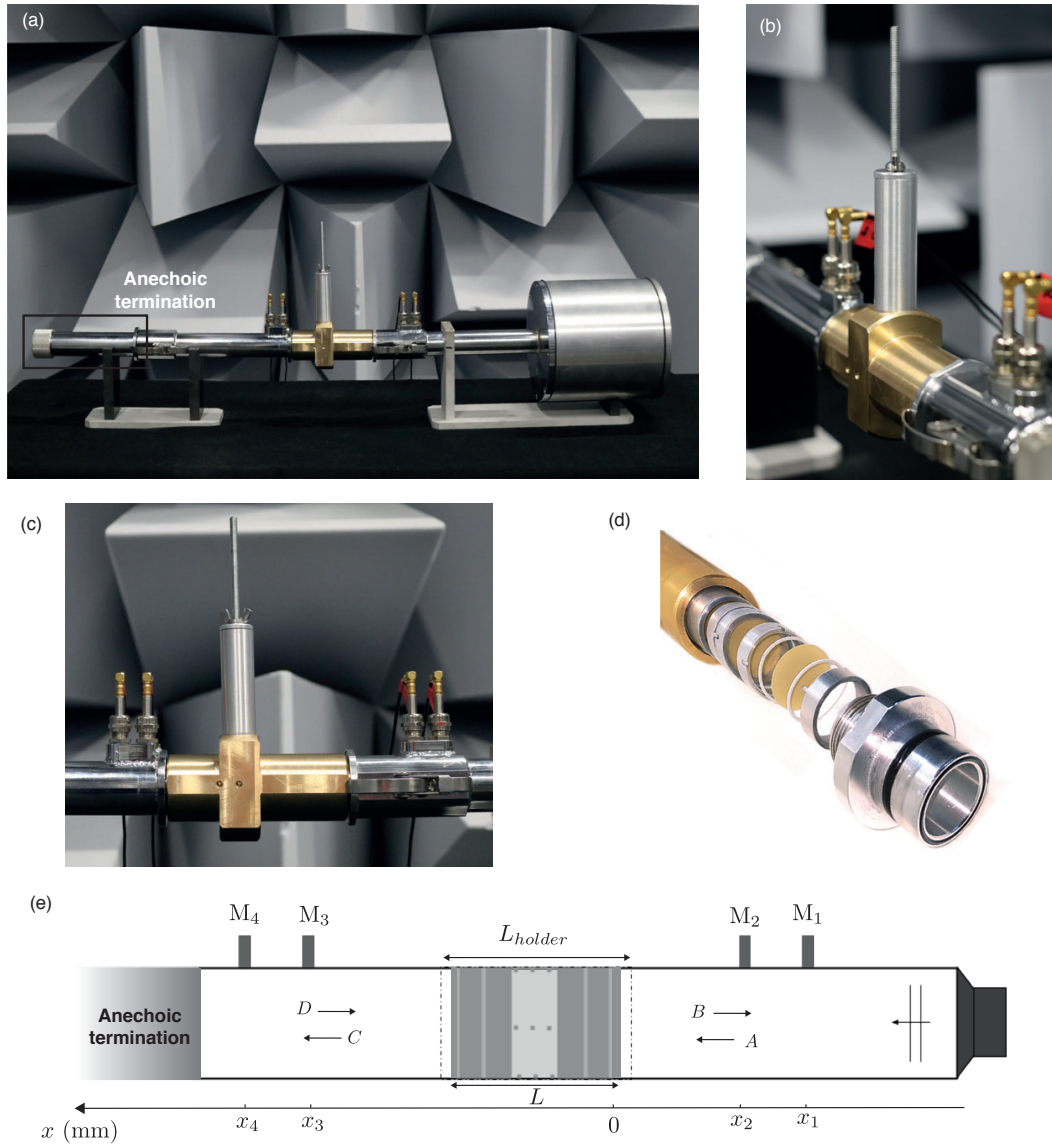


FIG. 1. [Color online] Experimental set-up photographs (a-d), sketch (e)

## II. ANALYTICAL MODEL

A transfer matrix method (TMM) is applied. A plane wave excitation at the input of the waveguide is assumed (i.e., the study is performed at frequencies lower than the first cut-off frequency of the circular waveguide). Thus, the system is 1-dimensional and reciprocal. The metamaterial can be considered as an equivalent medium since the wavelength remains much larger than its total length  $L$  at the working frequency range.

### A. Plate-type metamaterials analytical model

The proposed metamaterial consists of a periodic arrangement of circular clamped plates embedded in an air-filled cylindrical waveguide of radius  $R_a$  (cross section  $S = \pi R_a^2$ ), with a periodicity  $L_{unit} = L_{gap} + h$ , being  $L_{gap}$  the length of the air cavity on each side of the plate and  $h$  the thickness of the plate,

The plate elementary transfer matrix is given by  $\mathbf{T}_p = \begin{bmatrix} 1 & Z_p \\ 0 & 1 \end{bmatrix}$  with

$$Z_p = \frac{\Delta P}{SV} = -\frac{i\omega m I_1(k_p R_a) J_0(k_p R_a) + J_1(k_p R_a) I_0(k_p R_a)}{S^2 I_1(k_p R_a) J_2(k_p R_a) - J_1(k_p R_a) I_2(k_p R_a)}, \quad (\text{S1})$$

the Kirchhoff-Love thin plate acoustic impedance<sup>1</sup> where  $k_p = \omega^2 \sqrt{\rho_p h / D}$  is the wavenumber of the flexural waves excited in plate, with  $\rho_p$ ,  $h$  and  $D$  the density, the thickness and the bending rigidity of the plate respectively. The mass of the circular plate is  $m = \rho_p S h$ .

### B. Dopant analytical model

A Helmholtz resonator is used to dope the system. The corresponding elementary transfer matrix is given by

$$\mathbf{T}_{HR} = \begin{bmatrix} 1 & 0 \\ 1/Z_{HR} & 1 \end{bmatrix}, \quad (\text{S2})$$

with

$$Z_{HR} = \frac{1 \cos(k_n L_n) \cos(k_c L_c) - Z_n k_n \Delta L \cos(k_n L_n) \sin(k_c L_c) / Z_c - Z_n \sin(k_n L_n) \sin(k_c L_c) / Z_c}{i \sin(k_n L_n) \cos(k_c L_c) / Z_n - k_n \Delta L \sin(k_n L_n) \sin(k_c L_c) / Z_c + \cos(k_n L_n) \sin(k_c L_c) / Z_c}, \quad (\text{S3})$$

the impedance of the Helmholtz resonator, where  $\Delta L$  stands for the correction length of the neck accounting for the radiation at both ends

$$\Delta L = 0.82 \left[ 1 - 1.35R_n/R_c + 0.31 (R_n/R_c)^3 \right] R_n \quad (\text{S4})$$

$$+ 0.82 \left[ 1 - 0.235R_n/R_a - 1.32 (R_n/R_a)^2 + 1.54 (R_n/R_a)^3 - 0.86 (R_n/R_a)^4 \right] R_a. \quad (\text{S5})$$

### C. Total transfer matrix

The total transfer matrix  $\mathbf{T}$  of the  $N$  unit cells metamaterial, with a dopant element placed in the middle, takes the form

$$\begin{bmatrix} p \\ VS \end{bmatrix}_{z=0} = \mathbf{T} \cdot \begin{bmatrix} p \\ VS \end{bmatrix}_{z=L} \quad (\text{S6})$$

$$= (\mathbf{T}_{\text{cav}} \cdot \mathbf{T}_{\text{p}} \cdot \mathbf{T}_{\text{cav}})^{N/2} \cdot \mathbf{T}_{\text{HR}} \cdot (\mathbf{T}_{\text{cav}} \cdot \mathbf{T}_{\text{p}} \cdot \mathbf{T}_{\text{cav}})^{N/2} \cdot \begin{bmatrix} p \\ VS \end{bmatrix}_{z=L}, \quad (\text{S7})$$

$$(\text{S8})$$

with  $\mathbf{T}_{\text{cav}}$ , is the cavity transfer matrix in the air cavities,

$$\mathbf{T}_{\text{cav}} = \begin{bmatrix} \cos \frac{k_0 L_{\text{gap}}}{2} & iZ_0 \sin \frac{k_0 L_{\text{gap}}}{2} \\ \frac{i}{Z_0} \sin \frac{k_0 L_{\text{gap}}}{2} & \cos \frac{k_0 L_{\text{gap}}}{2} \end{bmatrix}, \quad (\text{S9})$$

where the subscript 0 and  $m$  are referring to the air medium and to the plate respectively,  $k$  represents the wave number,  $Z = \rho c/S$  the characteristic impedance,  $c$  the sound speed and  $\rho$  the mass density.

Visco-thermal losses accounting for the friction in the vicinity of the guide walls, within the viscous penetration thickness  $\delta_v = \sqrt{2\mu/\rho_0}$  (with  $\mu$  the dynamic viscosity coefficient,  $\rho_0$  the air density), are modeled by complex wave numbers  $k_0(\omega)$  and impedance  $Z_0(\omega)$ , as defined by Zwikker and Kosten<sup>4,5</sup>

$$k_0(\omega) = \frac{\omega}{c_0} \left( 1 + \frac{(1-i)}{\sqrt{2}R_a/\delta_v} \frac{(1+(\gamma-1))}{\sqrt{Pr}} \right), \quad (\text{S10})$$

$$Z_0(\omega) = \frac{\rho_0 c_0}{\pi R_a^2} \left( 1 + \frac{(1-i)}{\sqrt{2}R_a/\delta_v} \frac{(1-(\gamma-1))}{\sqrt{Pr}} \right), \quad (\text{S11})$$

with  $Pr$  the Prandtl number,  $\gamma$  the air heat capacity ratio and  $c_0$  the air velocity.

## D. Scattering parameters

As the system is reciprocal, the scattering parameters, i.e., transmission and reflection coefficients, are given by

$$R = \frac{T_{11} + T_{12}/Z_0 - Z_0 T_{21} - T_{22}}{T_{11} + T_{12}/Z_0 + Z_0 T_{21} + T_{22}}, \quad (\text{S12})$$

$$T = \frac{2}{T_{11} + T_{12}/Z_0 + Z_0 T_{21} + T_{22}}, \quad (\text{S13})$$

for symmetric systems, and

$$T = \frac{2}{T_{11} + T_{12}/Z_0 + Z_0 T_{21} + T_{22}}, \quad (\text{S14})$$

$$R^+ = \frac{T_{11} + T_{12}/Z_0 - Z_0 T_{21} - T_{22}}{T_{11} + T_{12}/Z_0 + Z_0 T_{21} + T_{22}}, \quad (\text{S15})$$

$$R^- = \frac{-T_{11} + T_{12}/Z_0 - Z_0 T_{21} + T_{22}}{T_{11} + T_{12}/Z_0 + Z_0 T_{21} + T_{22}}, \quad (\text{S16})$$

for asymmetric systems, with  $R^+$  the reflection coefficient for a left hand side incident wave, and  $R^-$  for a right hand side one.

The effective parameters of the periodic arrangement of plates are recovered from the  $\mathbf{T} = \mathbf{T}_{\text{cav}} \mathbf{T}_p \mathbf{T}_{\text{cav}}$  matrix of the unit cell such that

$$k(\omega) L_{\text{unit}} = \frac{\omega}{c(\omega)} L_{\text{unit}} = \cos^{-1} \left( \frac{T_{11} + T_{22}}{2} \right), \quad (\text{S17})$$

and

$$Z(\omega) = \sqrt{\frac{T_{12}}{T_{21}}} = \frac{\rho(\omega) c(\omega)}{S}. \quad (\text{S18})$$

## III. EXPERIMENTAL RECONSTRUCTION OF $R$ AND $T$

Acoustics pressure fields  $P_1$ ,  $P_2$  (microphones  $M_1$  and  $M_2$ , Fig. 1) and  $P_3$ ,  $P_4$  ( $M_3$  and  $M_4$ ), obtained from the frequency response measurements and the relative sensibilities between microphones  $M_2$ ,  $M_3$ ,  $M_4$  and the reference one  $M_1$

$$P_1 = (Ae^{-ikx_1} + Be^{ikx_1})e^{i\omega t}, \quad (\text{S19})$$

$$P_2 = (Ae^{-ikx_2} + Be^{ikx_2})e^{i\omega t}, \quad (\text{S20})$$

$$P_3 = (Ce^{-ikx_3} + De^{ikx_3})e^{i\omega t}, \quad (\text{S21})$$

$$P_4 = (Ce^{-ikx_4} + De^{ikx_4})e^{i\omega t}, \quad (\text{S22})$$

can be decomposed into incoming ( $A$  et  $D$ ) and outgoing ( $B$  et  $C$ ) waves from the metamaterial<sup>2,3</sup>

$$A = i \frac{P_1 e^{ikx_2} - P_2 e^{ikx_1}}{2 \sin k(x_1 - x_2)}, \quad (\text{S23})$$

$$B = i \frac{P_2 e^{-ikx_1} - P_1 e^{-ikx_2}}{2 \sin k(x_1 - x_2)}, \quad (\text{S24})$$

$$C = i \frac{P_3 e^{ikx_4} - P_1 e^{ikx_3}}{2 \sin k(x_3 - x_4)}, \quad (\text{S25})$$

$$D = i \frac{P_4 e^{-ikx_3} - P_3 e^{-ikx_4}}{2 \sin k(x_3 - x_4)}. \quad (\text{S26})$$

$$(\text{S27})$$

$A, B, C$  and  $D$  are linked to the transmission  $T$  and reflection  $R$  coefficients through the scattering matrix  $S$

$$\begin{bmatrix} B \\ C \end{bmatrix} = \begin{bmatrix} R & T \\ T & R \end{bmatrix} \begin{bmatrix} A \\ D \end{bmatrix}, \quad (\text{S28})$$

for symmetrical and reciprocal material.

The effective impedance can then be recovered from

$$Z(\omega) = Z_0 \sqrt{\frac{(1+R)^2 - T^2}{(1-R)^2 - T^2}}, \quad (\text{S29})$$

with

$$R = \frac{AB - CD}{A^2 - D^2}, \quad (\text{S30})$$

$$T = \frac{AC - BD}{A^2 - D^2}. \quad (\text{S31})$$

The effective wavenumber is obtained by inverting

$$e^{ik(\omega)L} = \frac{T(1 - Z(\omega)/Z_0)}{R(1 + Z(\omega)/Z_0) - Z(\omega)/Z_0 + 1}, \quad (\text{S32})$$

where  $L$  is the total length of the measured finite system, leading to

$$k(\omega) = -\frac{\ln(|e^{ik(\omega)L}|) + i \arg(e^{ik(\omega)L})}{iL} + \frac{2\pi n}{L}, \quad (\text{S33})$$

with  $n$  an integer accounting for the phase wrap due to the  $e^{ik(\omega)L}$  inversion.

The effective density  $\rho(\omega)$  and Bulk modulus  $\kappa(\omega)$  can then be estimated from the effective impedance and wavenumber

$$\rho(\omega) = \frac{Z}{c(\omega)} = Z \frac{k(\omega)}{\omega}, \quad (\text{S34})$$

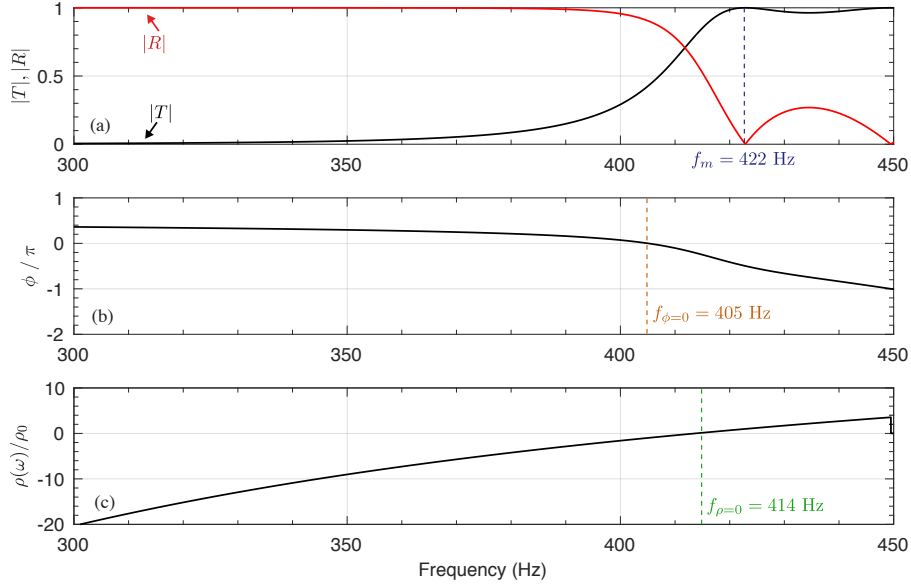


FIG. 2. [Color online] Scattering parameters of a lossless PAM composed of 20 plastic shims spaced by a distance  $L_{unit} = 1$  cm. Transmission (black color) and reflection coefficients (red color) (a), phase of the transmission coefficient (b), and real part of the effective density (c)

and

$$\kappa(\omega) = \rho(\omega)c(\omega)^2 = Z(\omega)\frac{\omega}{k(\omega)}, \quad (\text{S35})$$

Measurements are conducted in a temperature-controlled room so as to limit the impact of weather fluctuation on the measurements.

### A. Analytical scattering predictions of a lossless 20 PAM

We consider a periodic arrangement of  $N = 20$  thin elastic plastic shims (Young modulus  $E = 4.6$  GPa, density  $\rho = 1400$  kg.m<sup>-3</sup>, Poisson ratio  $\nu = 0.41$ , thickness  $h = 102$   $\mu$ m) equally spaced by a distance  $L_{gap} = 1$  cm and plugged into a circular waveguide of radius  $R_a = 15$  mm.

The analytical predictions in Fig. 2 are found using the aforementioned Transfer Matrix model.

Impedance matching (zero reflection, total transmission), zero-density, and zero-phase propagation occur at three different frequencies, respectively  $f_m = 422$  Hz,  $f_{\rho=0} = 414$  Hz, and  $f_{\phi=0} = 405$  Hz.

It is worth noting here that the dynamic bulk modulus and the effective dynamic mass density at  $f_{\phi=0}$  are  $\kappa(\omega) = 0.142$  MPa  $\approx \kappa_0$  and  $\rho(\omega) = -1.18$  kg.m<sup>-3</sup>  $\approx \rho_0$  respectively while at  $f_m$

they are  $\kappa(\omega) = 0.142 \text{ MPa} \approx \kappa_0$  and  $\rho(\omega) = 1.17 \text{ kg.m}^{-3} \approx \rho_0$ .

As opposed to  $f_m$  where the effective impedance is equal to that of air, i.e.,  $Z(\omega) = Z_0$  and

$$T = \frac{2}{2 \cos(k(\omega)L) - i \left[ \frac{Z(\omega)}{Z_0} + \frac{Z_0}{Z(\omega)} \right] \sin(k(\omega)L)} \quad (\text{S36})$$

$$= \frac{2}{2 \cos(k_0L) - i \left[ \frac{Z_0}{Z_0} + \frac{Z_0}{Z_0} \right] \sin(k_0L)} = e^{ik_0L} \rightarrow |T|_{|f_m} = 1, \quad (\text{S37})$$

at  $f_{\phi=0}$  the effective impedance,  $Z(\omega) = \sqrt{\kappa(\omega)\rho(\omega)}$ , is purely imaginary in the lossless case  $\text{Re}(Z(\omega)) = 0$  and  $\text{Im}(Z(\omega)) \approx Z_0$ , i.e.,  $Z(\omega) = iZ_0$  and

$$T = \frac{2}{2 \cos(k(\omega)L) - i \left[ \frac{Z(\omega)}{Z_0} + \frac{Z_0}{Z(\omega)} \right] \sin(k(\omega)L)} \quad (\text{S38})$$

$$= \frac{2}{2 \cos(ik_0L) - i \left[ \frac{iZ_0}{Z_0} - \frac{iZ_0}{Z_0} \right] \sin(ik_0L)} = \frac{1}{\cosh(k_0L)} \rightarrow |T|_{|f_{\phi=0}} \neq 1. \quad (\text{S39})$$

The impedance of the PAM is therefore not matched to that of the surrounding medium at the zero phase frequency, and unitary transmission is not achieved.

## B. Influence of the different loss sources

Figure 3 shows the scattering parameters of the system studied in figure 4 of the manuscript, accounting for the different sources of losses.

Figure 3(b) shows the transmission and reflection magnitude of the system when only viscothermal losses in the main waveguide are considered. In the frequency range of interest, and for the diameter of the main waveguide ( $d_a = 30 \text{ mm}$ ), the influence of viscothermal losses is almost imperceptible since we obtain almost the lossless scattering magnitude given in Fig. 3(a). The viscothermal losses in the Helmholtz resonator have a greater impact on the acoustic signature as can be seen in Fig. 3(c) since the neck dimensions are narrower ( $R_n = 2 \text{ mm}$ ). Friction occurs in the vicinity of the neck walls. Nevertheless, it should be noted here that most of the losses are due to the plate's visco-elasticity. Figure 3(d) shows that adding the viscoelastic loss factor  $\beta$  to the analytical model results in a drop in transmission of about 40%.

The viscoelastic loss factor of the plates is characterized acoustically using a multi-objective optimization based on a least mean square procedure, the cost function of which is given by

$$\mathbb{C}(\rho_p, E_p, \beta, \nu_p) = \|R_{meas} - R_{TMM}\|^2 + \|T_{meas} - T_{TMM}\|^2, \quad (\text{S40})$$



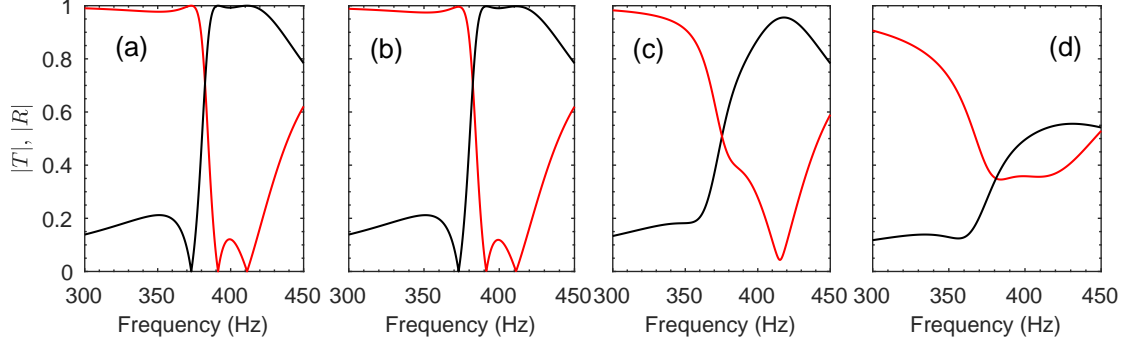


FIG. 3. Influence of viscothermal and viscoelastic losses: scattering parameters of a 6-unit long PAM doped with a Helmholtz resonator (a) with no losses, (b) with only the viscothermal losses in the main waveguide, (c) with the viscothermal losses in both the waveguide and the Helmholtz resonator, and (d) with all losses (viscothermal and viscoelastic).

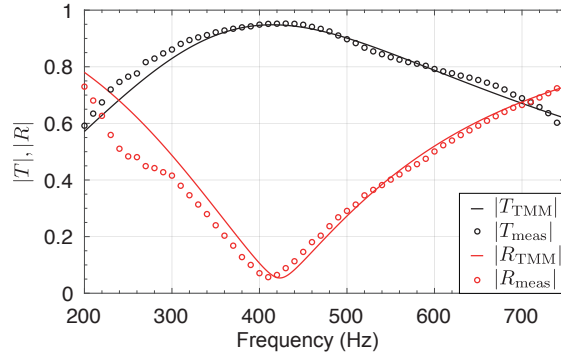


FIG. 4. Acoustic characterization of a single plate.

between the measured and analytical scattering coefficients of a single plate. Figure 4 shows the result of the characterization. A loss factor of  $\beta = 0.13$  is found.

#### IV. DERIVATION OF EQUATIONS 1 AND 2 OF THE MANUSCRIPT

The transmission coefficient of a layer of thickness  $L$  (with acoustic impedance  $Z(\omega) = \sqrt{\rho(\omega)\kappa(\omega)}$  and wavenumber  $k(\omega) = \omega\sqrt{\rho(\omega)/\kappa(\omega)}$ ) surrounded by air (with acoustic impedance  $Z_0$  and wave number  $k_0$ ) can be expressed as

$$T = \frac{2}{2 \cos(k(\omega)L) - i \left[ \frac{Z(\omega)}{Z_0} + \frac{Z_0}{Z(\omega)} \right] \sin(k(\omega)L)}. \quad (\text{S41})$$

The modulus and the phase of the transmission coefficient are then given by

$$|T| = \frac{2\sqrt{4\cos^2(k(\omega)L) + \left[\frac{Z(\omega)}{Z_0} + \frac{Z_0}{Z(\omega)}\right]^2 \sin^2(k(\omega)L)}}{4\cos^2(k(\omega)L) + \left[\frac{Z(\omega)}{Z_0} + \frac{Z_0}{Z(\omega)}\right]^2 \sin^2(k(\omega)L)}, \quad (\text{S42})$$

$$\phi = -\text{atan} \left( \frac{\left[\frac{Z(\omega)}{Z_0} + \frac{Z_0}{Z(\omega)}\right] \sin(k(\omega)L)}{2\cos(k(\omega)L)} \right), \quad (\text{S43})$$

thus leading to eq. (1-2) of the manuscript when rearranged

$$|T| = \left( \cos^2(\omega\sqrt{\rho CL}) + \frac{1}{4} \left[ \sqrt{\frac{\rho C_0 S_0}{C\rho_0 S}} + \sqrt{\frac{\rho_0 C S}{C_0\rho S_0}} \right]^2 \sin^2(\omega\sqrt{\rho CL}) \right)^{-1/2}, \quad (\text{S44})$$

$$\phi = -\text{atan} \left( \frac{1}{2} \left[ \sqrt{\frac{\rho C_0 S_0}{C\rho_0 S}} + \sqrt{\frac{\rho_0 C S}{C_0\rho S_0}} \right] \tan(\omega\sqrt{\rho CL}) \right), \quad (\text{S45})$$

When the density is exactly equal to zero,  $\rho = 0$ , Eq. (2) of the manuscript (Eq. (S45) of this supplemental) is undetermined, with  $\tan(\omega\sqrt{\rho CL}) = 0$  and  $\sqrt{C/\rho} \rightarrow \infty$ , and requires a passage to the limit, that is

$$\lim_{\varepsilon \rightarrow 0} \left( (\sqrt{\varepsilon}^{-1} + \sqrt{\varepsilon}) \tan(\sqrt{\varepsilon}) \right) = 1 + 4\varepsilon/3 + O(\varepsilon)^{3/2}.$$

Equation (2) then results in a non-zero constant phase at  $f_{\rho=0}$

$$\lim_{\rho(\omega) \rightarrow 0} -\text{atan} \left( \frac{1}{2} \left[ \sqrt{\frac{\rho C_0 S_0}{C\rho_0 S}} + \sqrt{\frac{\rho_0 C S}{C_0\rho S_0}} \right] \tan(\omega\sqrt{\rho CL}) \right) \neq 0.$$

## **V. DOPING VIDEOS**

## **ACKNOWLEDGMENTS**

This article is based upon work from COST Action DENORMS CA15125, supported by COST (European Cooperation in Science and Technology). This work has been funded by the Metaroom Project No. ANR-18-CE08-0021, co-funded by ANR and RCG.

## **REFERENCES**

<sup>1</sup>F. Bongard, H. Lissek, and J. R. Mosig, “Acoustic transmission line metamaterial with negative/zero/positive refractive index,” *Physical Review B - Condensed Matter and Materials Physics* **82**, 24–26 (2010).

- <sup>2</sup>B. H. Song and J. S. Bolton, “A transfer-matrix approach for estimating the characteristic impedance and wave numbers of limp and rigid porous materials,” *The Journal of the Acoustical Society of America* **107**, 1131–1152 (2000).
- <sup>3</sup>M. Niskanen, J. Groby, A. Duclos, O. Dazel, J. C. Le Roux, N. Poulain, T. Huttunen, and T. Lähivaara, “Deterministic and statistical characterization of rigid frame porous materials from impedance tube measurements,” *The Journal of the Acoustical Society of America* **2407** (2017), 10.1121/1.5008742.
- <sup>4</sup>C. Zwikker and C. W. Kosten, “Sound absorbing materials,” (1949).
- <sup>5</sup>M. R. Stinson, “The propagation of plane sound waves in narrow and wide circular tubes, and generalization to uniform tubes of arbitrary cross-sectional shape,” *J. Acoust. Soc. Am* **89** (1991), 10.1121/1.400379.